The Resistance to Cavitation Erosion of CrMnN Stainless Steels

W.T. Fu, Y.B. Yang, T.F. Jing, Y.Z. Zheng, and M. Yao

(Submitted 20 May 1996; in revised form 28 May 1998)

The resistance to cavitation erosion (CE) was measured using a magnetostrictive device and a rotating disk device for some CrMnN stainless steels (Chinese patent ZL 90 1 02197.0). The microstructural changes in the surface layer before and after CE were analyzed by use of Mossbauer spectra. Results show that the resistance to CE of duplex austenitic-martensitic CrMnN stainless steels is much better than that of ZG0Cr13Ni4-6Mo and ZG0Cr16Ni5Mo steel, which are in common use for hydraulic turbine runners. The metastable austenite and its changes in the process of CE are the key factors why the CrMnN stainless steels have excellent resistance to cavitation erosion.

Keywords austenite, cavitation erosion, CrMnN steels, hydraulic turbines, Mossbauer spectra

1. Introduction

Cavitation erosion and sandy wear erosion are worldwide problems because they degrade hydraulic turbine runners. (A runner is a part of the hydraulic turbine. It rotates during operation. Cavitation erosion is a major failure mechanism of the runner.) They seriously reduce the service life, service capability of the devices, and the output and economics of the hydropower stations (Ref 1, 2). In order to minimize the damage and to solve the problem, more and more attention has been given to developing CE-resistant materials in material science and engineering fields over the last decades. The CrNiMo stainless steels (such as ZG0Cr13Ni4-6Mo and ZG0Cr16Ni5Mo) developed in the 1960s have much better resistance to CE than conventional materials. They contain a more expensive rare metal (nickel), so it is important to develop the cheaper CrMnN stainless steels for the hydraulic turbines. This article analyzes the structural changes of the CrMnN stainless steels before and after CE by the use of Mossbauer spectra, and discusses the reasons why they have improved resistance to CE.

W.T. Fu, T.F. Jing, Y.Z. Zheng, and **Y. B. Yang,** Department of Materials Engineering, Yanshan University, Qinhuangdao, 066004, China; **M. Yao,** Harbin Institute of Technology, Harbin, China. **W.T. Fu** is also associated with the Harbin Institute of Technology; **Y.B. Yang** is also associated with the Bohai Aluminum Industries Co., Ltd., Qinhuangdao, China.

2. Materials and Methods

Three kinds of CrMnN stainless steels that contain different amount of manganese and nitrogen were used as test materials. Their chemical compositions are shown in Table 1. The CrNiMo steels that are in common use currently for runners were also tested for their resistance to CE. Heat treatment conditions and microstructures of all these materials before CE testing are summarized in Table 2.

The dimensions of the specimens for vibratory and rotating disk CE tests are shown in Fig. 1. Before CE testing, the specimens were electropolished with a solution that was 20% perchloric acid in ethanol at 18 V.

CE tests were conducted on a J93025 model ultrasonic vibratory magnetostrictive device (at a frequency of 19.7 kHz and an amplitude of 42 μm), and on a N-CA model rotating disk device (in which the pressure was 0.102 MPa, linear velocity was 45 m/s, and the hole of the CE inducer was 16 mm in diameter) in tap water at ambient temperature.

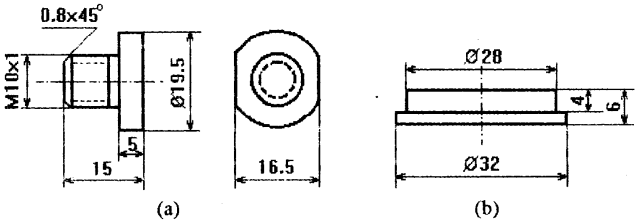

Fig. 1 Geometry and dimensions of CE test specimens. (a) Vibratory CE. (b) Rotating disk CE

Table 1 Chemical composition of the materials used in corrosion-erosion tests

Materials	Steel	Composition, wt% C	Mn	Cr	N	Ni	Mo	S	P
CrMnN	T1	0.036	6.71	13.21	0.06	…	0.24	0.004	0.018
	T2	0.050	7.80	13.14	0.07	…	0.32	0.004	0.017
	T3	0.050	9.60	13.03	0.10	…	0.38	0.004	0.018
CrNiMo	C1	0.050	1.27	13.98	…	4.80	0.50	0.003	0.018
	C2	0.034	0.36	11.90	…	6.10	0.64	0.002	0.018
	C3	0.050	0.45	15.00	…	5.00	0.59	0.004	0.019

An AME-50 model Mossbauer spectrometer (Tsinghua University, Beijing, China) was used to study the structural changes of surface layer of the specimens after the CE test. The ^{57}Co acts as the radioactive source for the Mossbauer spectrometer, and rhodium acts as the substrate. The detector is a proportional airflow counter (90% He + 10% CH_4), using αFe to calibrate the scale of velocity. The gas velocity is at 35 bubble/min, and the high voltage is at 1500 V. The least squares fit was utilized for regression analysis of the spectra.

Table 2 Heat treatment regimes of the testing steels and their microstructures

Heat treatment regime	Steel	Microstructure
Solutionizing at 1050 °C for 1.5 h + air cooling + tempering at 500 °C for 2 h	T1	100% M
	T2	82% M + 18% A
	T3	63% A + 37% M
Solutionizing at 1000 °C + tempering for 1 h at:		
620 °C and 590 °C	C1	M + F
600 °C and 580 °C	C2	M + A_R
600 °C	C3	M + F

M, martensite; A, austenite; F, ferrite; A_R, retained austenite

3. Experimental Results

3.1 Results of CE Tests

The curves of weight loss versus exposure time (vibratory CE) are shown in Fig. 2. The longer the exposure time is, the greater the total weight loss is for every steel. The best one is T3 steel.

Figures 3(a) and (b) show the curves of the total weight loss and CE rate versus exposure time of T3, C1, C2, and C3 steel under the same conditions (rotating disk CE). Table 3 indicates

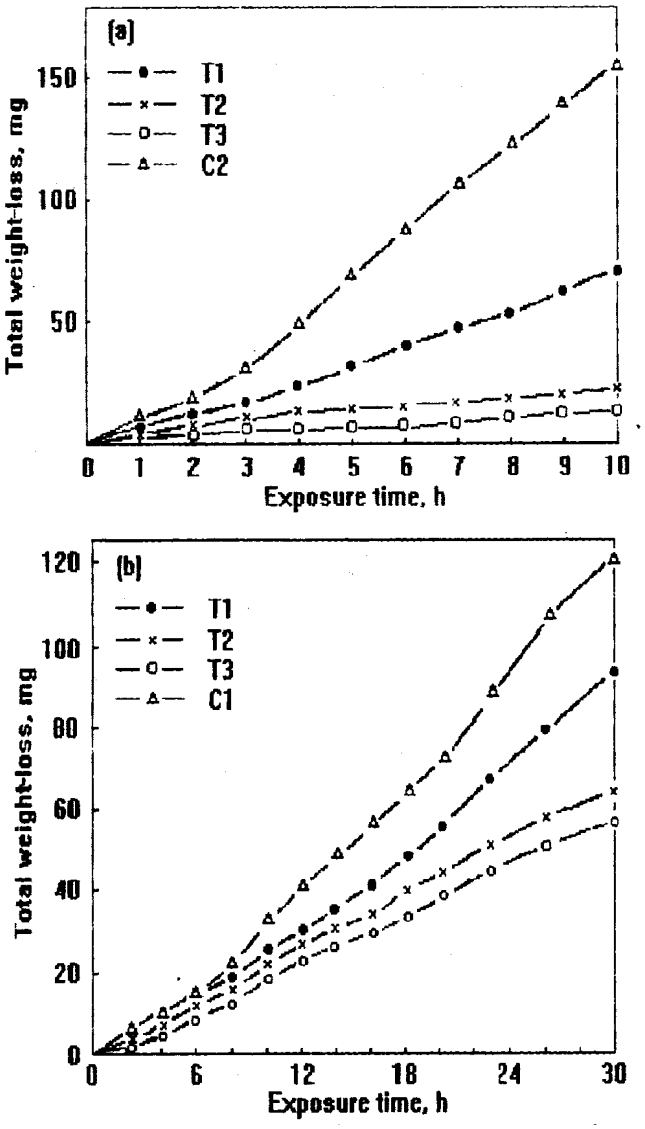

Fig. 2 Curves for total weight loss vs. exposure. (a) Vibratory CE. (b) Rotating disk CE (water with sand of Yellow River)

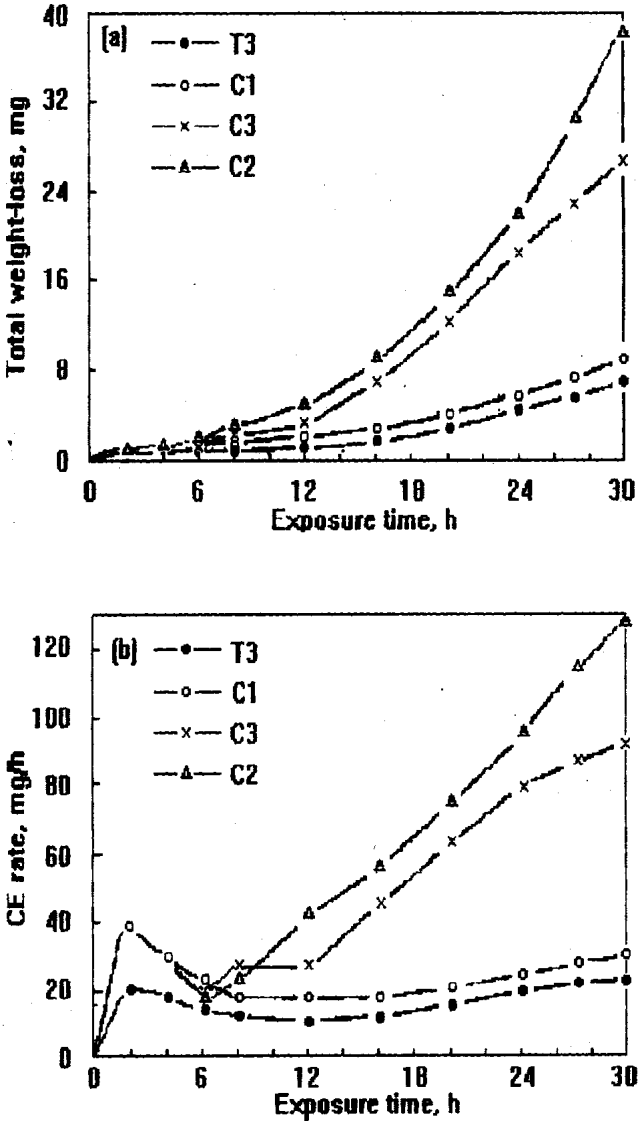

Fig. 3 Curves of total weight loss and CE rate vs. exposure time (rotating disk CE). (a) Weight loss curve. (b) CE rate curve

that T3 steel has not only the lowest weight loss and the longest incubation period of CE, but also the lowest CE rate in the accumulation period (the period after the incubation period in the CE rate curve). It also has the lowest average rate of CE compared with other steels. All the CE-resistant indexes of T3 steel are superior to that of the others.

3.2 Results of the Mossbauer Spectra Analysis

In the Mossbauer experiment, the examined thickness of the surface layer is less than 1 μm. However, the CE eroded depth is in the range between several microns to several centimillimeters (Ref 3). Therefore, we think that the examined depth of the Mossbauer experiment is completely in the range of the CE effected zone.

After the vibratory CE for different times, a series of changes of phase distribution and microstructure took place on the surface layer of the T3 steel specimens. Figures 4(a) to (d) are the Mossbauer spectra corresponding to the conditions before CE (0 h) and after CE at 2 h, 6.75 h, and 10 h. Table 4 contains a summary of the corresponding Mossbauer spectra parameters. In Fig. 4, the middle peak in every spectrum is a paramagnetic single peak of austenite, and the others are the six line peaks of martensite.

Table 4 and Fig. 4 show that the microstructure of the surface layer of the specimens before and after CE consists of austenite and martensite. There exist two kinds of martensite, M1 and M2, whose H_{hf} values are 294 kOe and 265 kOe before testing, respectively. The total amount of martensite increases with the exposure time, and a new kind of martensite, M3, whose H_{hf} value is 232 kOe is introduced.

4. Discussion

In the process of CE, the collapse of cavities can generate a high impact stress more than several hundred, or even several thousand, megabar (Ref 4), and the small area of material surface is subjected to deformation and damage. If the microstructure of the material is stable (e.g. martensite), CE only leads to the increase in dislocation density, hydraulic impact hardening, and peeling of the surface layer (Ref 5). In initial stages (incubation period) of CE, the plastic deformation only takes place on the surface of the specimen. After that, in addition to plastic deformation, the debris peelings occur in many local zones and spread over the surface (Ref 6). Among CrMnN steels, the average CE rate decreases with the increase of initial austenite amount, so analyzing the behavior of the austenite under CE conditions is essential for us to reveal the interactive mechanism between austenite and impact caused by collapse cavities.

In the present investigation, T3 steel has the largest amount of initial austenite, and the most impact strain energy of CE was

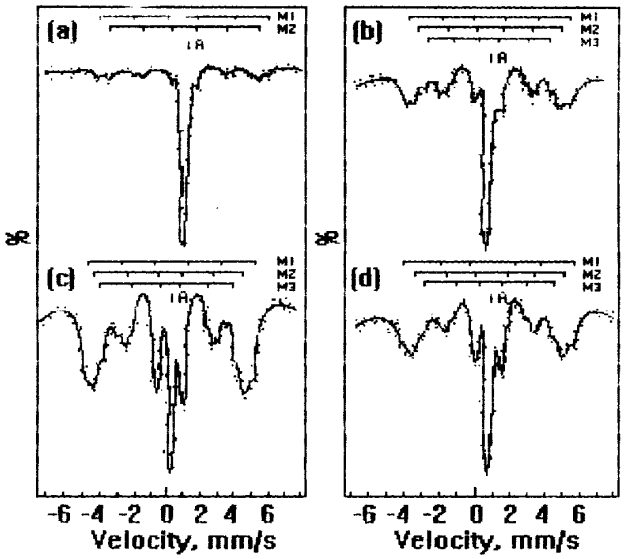

Fig. 4 Mossbauer spectra of surface layer specimens under different CE conditions. (a) Before CE. (b) CE for 2 h. (c) CE for 6.75 h. (d) CE for 10 h

Table 3 Summary of comparison of CE-resistant indexes

Materials	Total weight loss, mg	Incubation period of CE, h	CE rate in accumulation period, mg/h	Average CE rate, mg/h
T3	7.20	16.90	0.33	0.24
C1	8.70	12.15	0.39	0.29
C2	39.00	9.00	1.57	1.30
C3	27.60	9.00	1.22	0.92

All tests were carried out for 30 h.

Table 4 Parameters of Mossbauer sprectra under different CE conditions for T3 steel

	Martensite						Austenite	
	M1		M2		M3		A	
Exposure time, h	H_{hf}, kOe	f, wt%	H_{hf}, kOe	f, wt%	H_{hf}, kOe	f, wt%	Is, mm/s	f, wt%
0	294	15.82	265	20.98	…	…	–0.37821	63.20
2	292	53.62	262	15.72	231	4.55	–0.40410	26.11
6.75	294	39.00	265	36.82	233	11.9	–0.37554	12.27
10	293	26.6	266	52.82	232	10.15	–0.38096	18.33

H_{hf}, hyperfine effective magnetic field; f, fractional amount of each phase in the top-most surface layer; Is, isomer shift

absorbed before peeling fracture of the debris formed by repeating impact of cavitation. Undoubtedly, austenite itself is one of the major reasons that T3 steel shows the highest resistance to CE.

On the other hand, in the process of CE, the collapse of cavities near the specimen surface can generate a very high impact stress: more than several hundreds, or even several thousands, of megapascals. This strong impact on the surface layer of the T3 specimen can also be relaxed by the transformation of austenite to martensite (γ/α'). Figure 4 and Table 4 show that the amount of α'-martensite induced by CE increases with the exposure time to CE. At the same time, changes of hyperfine structure inside martensite occur also. The atomic configuration around the ^{57}Fe nuclei in M1, M2, and M3 are quite different; hence, the appearance of M3 and the change in relative fractions of M1, M2, and M3 indicate both the phase transformation and the atomic configuration change in the process of CE (Ref 7). Therefore, it is necessary to consume or absorb the impact energy of CE as the driving force of the microstructural changes.

In short, all the behaviors of initial austenite in the CrMnN steel during CE (such as the deformation, work-hardening, martensitic transformation, and reconfiguration of alloying element atoms in the phase) delay debris peeling, so that there is always a new hardening layer to resist the damage of CE. The CrNiMo steels are already martensite and contain little, if any, austenite that can be available for transformation. However, there are not similar behaviors of austenite in the CrNiMo steels; thus all the CE impact energy mainly acts on the surface martensite layer.

5. Conclusions

- The CrMnN stainless steels have much better resistance to CE than ZG0Cr13Ni4-6Mo and ZG0Cr16Ni5Mo, which are commonly used for hydraulic turbine runners.
- The resistance to CE of the CrMnN stainless steels links much more to the amount of metastable austenite; the more austenite, the more impact energy absorbed before peeling.
- Work-hardening, strain-induced martensite transformation, and stress relaxation, as well as the reconfiguration of the alloying element atoms around ^{57}Fe nuclei in the process of CE, are the key factors influencing why the CrMnN duplex austenitic-martensitic stainless steels have excellent resistance to CE.

Acknowledgment

The authors are grateful to Mr. X.K. He for experimental assistance.

References

1. A. Karimi and J.L. Martin, *Int. Met. Rev.*, Vol 31, 1986, p 1
2. S.H. Gu, *Technology on Great Motor,* Vol 3, 1982, p 48 (in Chinese)
3. A. Karimi, Strength of Metals and Alloys, *Proceedings of the 7th International Conference on the Strength of Metals and Alloys*, Pergamon Press, Vol 2, J.J. McQueen et al., Ed., 12-16 Aug 1985, p 1607-1612
4. B. Vyas and C.M. Preece, *J. Appl. Phys.*, Vol 47 (No. 12), 1976, p 5133-5138
5. X.Y. Liu and N.Y. Tang, *Collections of Examples in Wear-Failure Analysis*, Mechanical Industry Press, Beijing, 1985, p 282 (in Chinese)
6. J.S. Change, M.S. Shou, and X.Z. Yu, Running of Hydraulic Turbine, Hydro-Electric Power Industry Press, 1983, p 22 (in Chinese)
7. W.T. Fu, Y.Z. Zheng, and T.F. Jing, *Progression in Natural Science*, Science Press, P.R. China, Vol 2, 1992, p 521 (in Chinese)